Article

Cell Reports

Mitochondrial ROS Production Protects the Intestine from Inflammation through Functional M2 Macrophage Polarization

Graphical Abstract

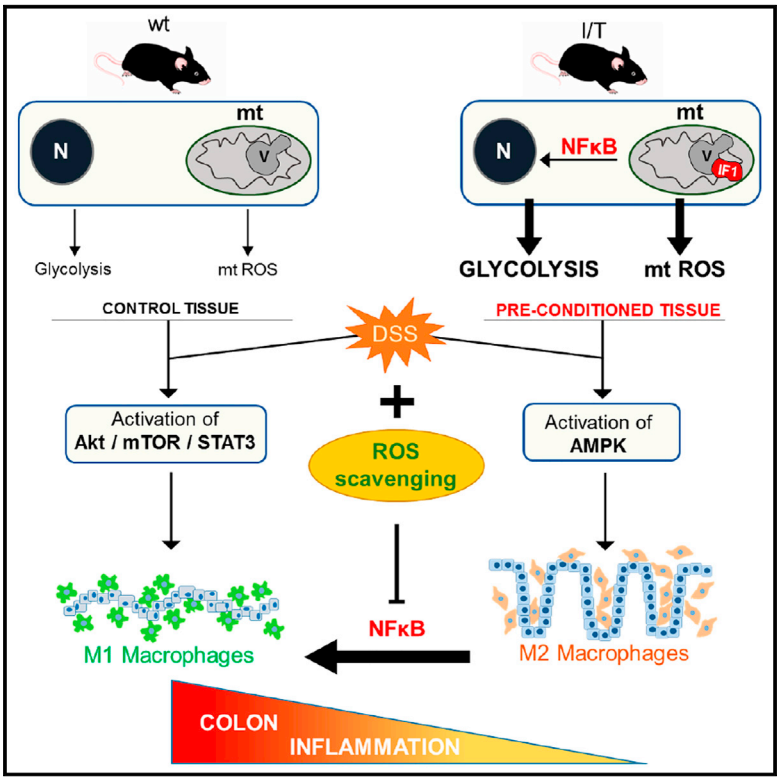

Highlights

- ATP-synthase inhibition induces anti-inflammatory pre-conditioning in the intestine
- Preconditioning is exerted by mitochondrial-ROS-dependent activation of NFκB
- Tissue-derived mtROS recruit and polarize macrophages to the M2 phenotype
- Quenching mtROS in vivo decreases NFκB-guided anti-inflammatory phenotype

Authors

Laura Formentini, Fulvio Santacatterina, Cristina Núñez de Arenas, ..., Ron Smits, Michael P. Murphy, José M. Cuezva

Correspondence

jmcuezva@cbm.csic.es

In Brief

Formentini et al. demonstrate in vivo how the mitochondrial production of ROS in the intestinal epithelium leads to NFκB activation and the protection from inflammation through the recruitment of M2-macrophages, linking mitochondrial activity to the innate immune response of the tissue microenvironment.

Formentini et al., 2017, Cell Reports *19*, 1202–1213
May 9, 2017
http://dx.doi.org/10.1016/j.celrep.2017.04.036

CellPress

OPEN ACCESS
CellPress

Cell Reports
Article

Mitochondrial ROS Production Protects the Intestine from Inflammation through Functional M2 Macrophage Polarization

Laura Formentini,[1,2,3] Fulvio Santacatterina,[1,2,3] Cristina Núñez de Arenas,[1,2,3] Konstantinos Stamatakis,[1] David López-Martínez,[1,2,3] Angela Logan,[4] Manuel Fresno,[1] Ron Smits,[5] Michael P. Murphy,[4] and José M. Cuezva[1,2,3,6,*]

[1]Departamento de Biología Molecular, Centro de Biología Molecular Severo Ochoa, Consejo Superior de Investigaciones Científicas-Universidad Autónoma de Madrid (CSIC-UAM), 28049 Madrid, Spain
[2]Centro de Investigación Biomédica en Red de Enfermedades Raras (CIBERER), ISCIII, 28049 Madrid, Spain
[3]Instituto de Investigación Hospital 12 de Octubre, Universidad Autónoma de Madrid, 28049 Madrid, Spain
[4]Medical Research Council Mitochondrial Biology Unit, Wellcome Trust/MRC Building, Cambridge CB2 0XY, UK
[5]Department of Gastroenterology and Hepatology, Erasmus MC-University Medical Center, 3000 Rotterdam, the Netherlands
[6]Lead Contact
*Correspondence: jmcuezva@cbm.csic.es
http://dx.doi.org/10.1016/j.celrep.2017.04.036

SUMMARY

Mitochondria are signaling hubs in cellular physiology that play a role in inflammatory diseases. We found that partial inhibition of the mitochondrial ATP synthase in the intestine of transgenic mice triggers an anti-inflammatory response through NFκB activation mediated by mitochondrial mtROS. This shielding phenotype is revealed when mice are challenged by DSS-induced colitis, which, in control animals, triggers inflammation, recruitment of M1 pro-inflammatory macrophages, and the activation of the pro-oncogenic STAT3 and Akt/mTOR pathways. In contrast, transgenic mice can polarize macrophages to the M2 anti-inflammatory phenotype. Using the mitochondria-targeted antioxidant MitoQ to quench mtROS in vivo, we observe decreased NFκB activation, preventing its cellular protective effects. These findings stress the relevance of mitochondrial signaling to the innate immune system and emphasize the potential role of the ATP synthase as a therapeutic target in inflammatory and other related diseases.

INTRODUCTION

Mitochondria are vital hubs in cellular physiology, playing essential roles in the control of energy production, intermediary metabolism, progression through the cell cycle, the execution of cell death, and signaling. The organelles have established pathways of communication with the nucleus and with other subcellular compartments to adapt cellular responses to different cues (Chandel, 2015; Quirós et al., 2016; Shadel and Horvath, 2015). This communication is exerted by a growing list of signaling molecules that include Ca^{2+}, various metabolites, and reactive oxygen species (ROS) (Glancy and Balaban, 2012; Sena and Chandel, 2012; Shi and Tu, 2015). Defective mitochondria have been implicated in inflammatory pathologies such as type 2 diabetes, Crohn's disease, and colon cancer (Galluzzi et al., 2012; Naik and Dixit, 2011; Weinberg et al., 2015). Inflammatory diseases are often characterized by excessive ROS production (Myant et al., 2013). Mitochondrial ROS (mtROS) have been suggested to act as signal-transducing molecules that trigger inflammation by driving pro-inflammatory cytokine production (Naik and Dixit, 2011). Indeed, mtROS and other metabolites derived from mitochondrial activity are critical elements for innate and adaptive immune responses (Colegio et al., 2014; O'Neill, 2014; Osborn and Olefsky, 2012; Weinberg et al., 2015; West et al., 2015).

The mitochondrial H^+-ATP synthase is the rotatory engine of the inner mitochondrial membrane that utilizes the proton electrochemical potential generated by the respiratory chain for the synthesis of ATP (Boyer, 1997). The activity of the H^+-ATP synthase is regulated by its physiological inhibitor, the ATPase Inhibitory Factor 1 (IF1). IF1 is known to block rotatory catalysis of the enzyme when mitochondria become depolarized (Gledhill et al., 2007). The interaction and inhibitory activity of IF1 on the ATP synthase is prevented by phosphorylation of S39 in IF1 by the action of a mitochondrial cyclic AMP (cAMP)-dependent protein kinase A (PKA) (García-Bermúdez et al., 2015). The overexpression of IF1, both in cell lines (Formentini et al., 2012; Sánchez-Aragó et al., 2013; Sánchez-Cenizo et al., 2010) and in hepatocytes (Santacatterina et al., 2016) and neurons (Formentini et al., 2014) of transgenic mice in vivo, also triggers the inhibition of the synthase by the overloading of the cells with the inhibitor. The inhibition of the ATP synthase by IF1 results in a mild ROS production that acts as a retrograde signal to the nucleus for the activation of different survival pathways (Formentini et al., 2012, 2014; Santacatterina et al., 2016). The availability of conditional transgenic mice that express human IF1 (hIF1) in a tissue-restricted way (Formentini et al., 2014; Santacatterina et al., 2016) provided the opportunity to test in vivo the relevance of the inhibition of the ATP synthase in inflammation and the immune response.

Herein, we have generated a mouse model expressing hIF1 in the intestinal epithelium to assess the physiological role of the ATP synthase in inflammation. The expression of hIF1

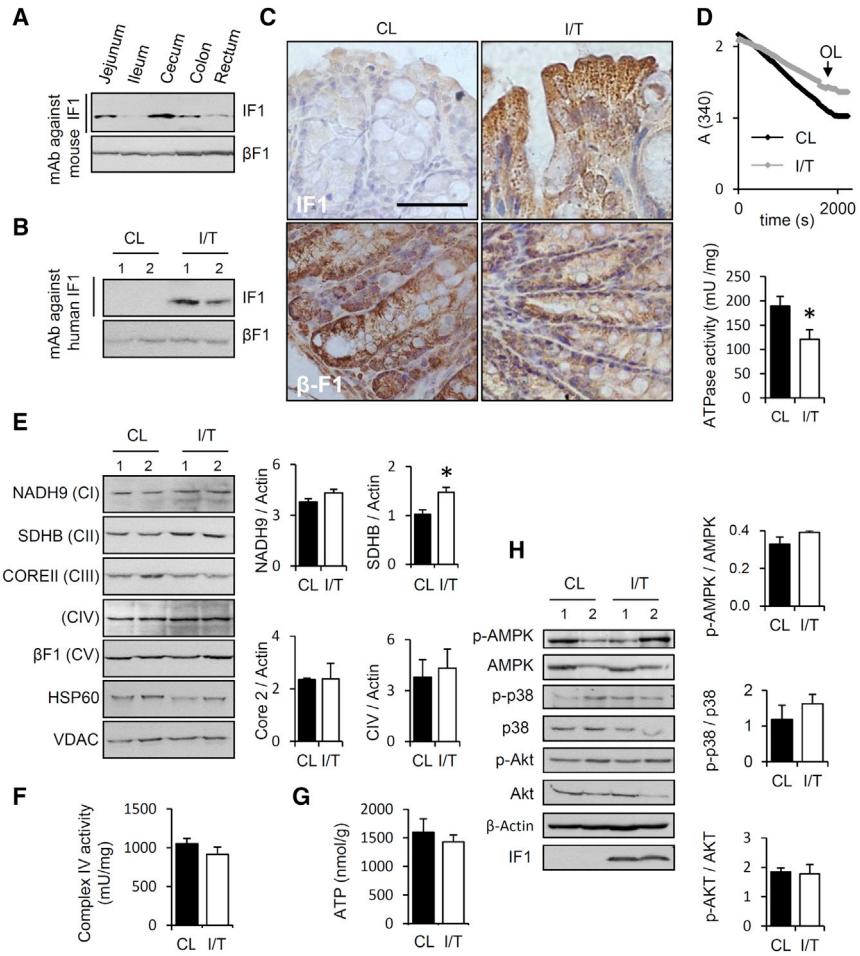

Figure 1. Characterization of Mice Expressing IF1 in Colon

(A) Western blots reveal the differential expression of mouse IF1 (12 kDa) in fractionated proteins from jejunum, ileum, cecum, colon, and rectum extracts. β-F1-ATPase (βF1) expression is shown as loading control. mAb, monoclonal antibody.

(B) Western blots of β-F1 and human IF1 in control (CL) and I/T mice.

(C) Immunohistochemistry reveals the granular cytoplasmic staining of human IF1 only in colons of I/T mice. β-F1 staining in control (CL) and I/T mice is also shown. Scale bar, 50 μm.

(D) Hydrolase activity of the ATP synthase in isolated colonocytes from control (CL, black trace) and I/T (gray trace) mice. Where indicated, 10 μM oligomycin (OL) was added. Histograms show the activity in colonocytes from control (CL, closed bar) and I/T (open bar) mice.

(E) Representative blots of mitochondrial proteins NADH9 (subunit of complex I), SDHB (subunit of complex II), COREII (subunit of complex III), COXIV (subunit of complex IV), and β-F1 (subunit of complex V) in control (CL) and I/T mice. Two colon samples per condition tested are shown. HSP60 and VDAC are shown as loading controls.

(F and G) Shown here, (F) cytochrome *c* oxidase activity and (G) ATP levels in isolated colonocytes from control (CL, closed bar) and I/T (open bar) mice.

(H) Blots of signaling kinases (phosphorylated [p]-AMPK, AMPK, p-p38, p38, p-AKT, and AKT) in colon extracts from control (CL) and I/T mice. Two colon samples per condition tested are presented. hIF1 is only expressed in I/T mice. β-actin is used as loading control.

In (D–H), histograms indicate the mean ± SEM of five mice per group assayed in duplicate. *$p < 0.05$, when compared to control by Student's t test.

See also Figure S5.

inhibits the activity of oxidative phosphorylation (OXPHOS), mediates the shift of colonocytes to an enhanced glycolysis, and prompts the stimulation of innate immunity through the activation of the AMPK (5′ AMP-activated protein kinase) pathway and the mtROS-mediated induction of nuclear factor κB (NFκB) signaling. This metabolic reprogramming affords protection against dextran sodium sulfate (DSS)-induced intestinal inflammation and is associated with the recruitment and polarization of intestinal macrophages to the M2 anti-inflammatory phenotype, a reduction in the production of pro-inflammatory cytokines, and a diminished tissue activation of mTOR (mammalian target of rapamycin) signaling. Overall, our findings provide in vivo evidence highlighting the H^+-ATP synthase as a target to prevent inflammation.

RESULTS

The Double-Transgenic I/T Mice Express hIF1 in the Intestine

To assess the in vivo role of IF1 in the intestinal epithelium, a transgenic Tet-On mouse model was developed. The endogenous expression of IF1 in mice intestine is variable (Figure 1A), being high in cecum, intermediate in colon, and negligible in ileum (Figure 1A). Double-transgenic mice (specifically, I/T mice) expressing hIF1 were obtained by breeding mice containing the human Tet-IF1-47 transgene (I) with mice expressing the intestine-specific Villin-rtTA2-M2 transactivator (T) (Roth et al., 2009). Western blotting (Figure 1B) and immunohistochemistry (Figure 1C) with a human-specific anti-IF1 antibody confirmed the expression of hIF1 in colon in response to the administration of doxycycline. Expression of hIF1 promoted a significant reduction in the ATPase activity (Figure 1D) but had no effect on the expression of several OXPHOS proteins (Figure 1E), with the exception of an increase in SDHB of complex II (Figure 1E). Interestingly, the expression of hIF1 in the intestine did not affect the activity of complex IV of the respiratory chain (Figure 1F). Consistent with hIF1 exerting a milder inhibition of the ATP synthase than H49K in vivo, we noted that I/T mice showed no relevant differences in the content of ATP in the intestine when compared to controls (Figure 1G). Likewise, none of the stress kinases induced by restraining the activity of the ATP synthase with H49K in liver and in brain (AMPK, p38 MAPK [mitogen-activated protein kinase], and Akt) (Formentini et al., 2014; Santacatterina et al., 2016) were affected by the expression of hIF1 in the intestine (Figure 1H).

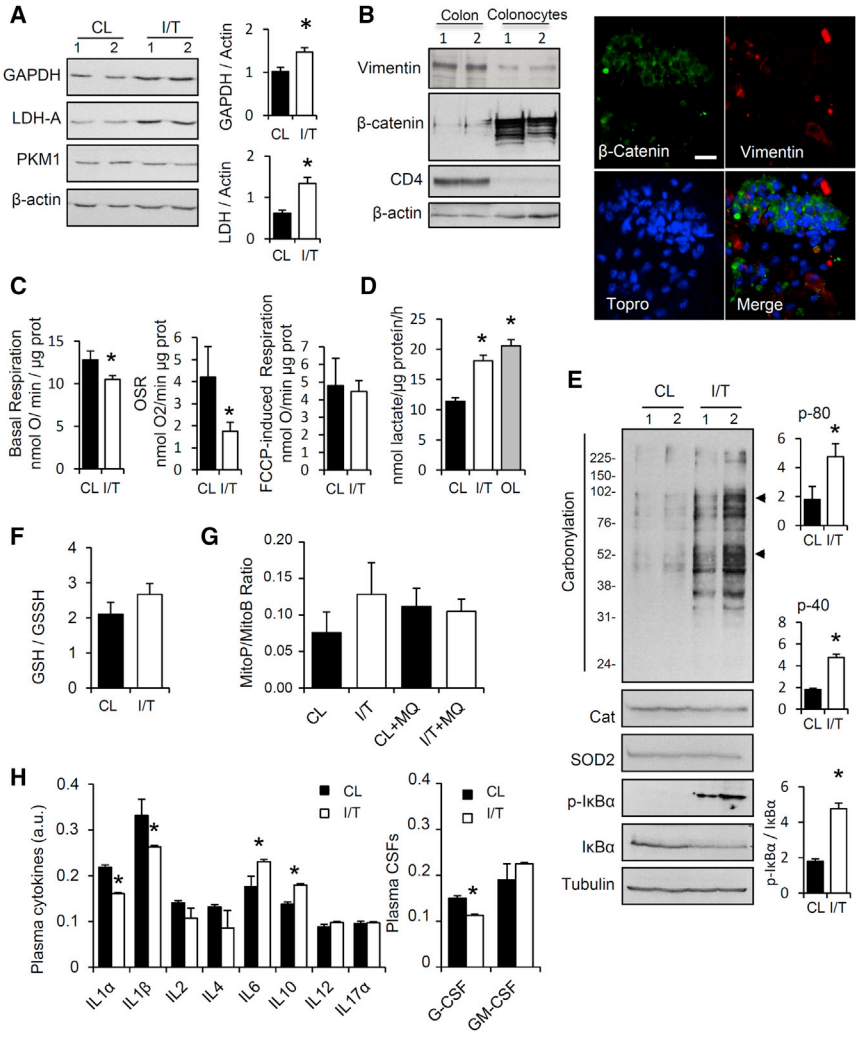

Figure 2. Expression of hIF1 Triggers Metabolic Reprogramming

(A) Western blots show the IF1-dependent increase in the glycolytic proteins LDH-A and GAPDH in two colon samples per condition tested. PKM1 and β-actin expression are also shown.

(B) Blots show the enrichment of β-catenin and impoverishment of vimentin and the CD4 (immune cell) marker in isolated colonocyte preparations. Immunofluorescence microscopy of colonocytes stained with anti-β-catenin (epithelial marker, green) and anti-vimentin (mesenchymal marker, red) antibodies. TOPRO staining (blue) identified nuclei. Scale bar, 20 μm.

(C) Polarographic determination of oxygen consumption rates in isolated colonocytes of control (CL, closed bars) and I/T (open bars) mice. The basal, oligomycin (OL)-sensitive (OSR) and FCCP-stimulated respiration are shown.

(D) Determination of lactate production in colonocytes of control (CL, closed bars) and I/T (open bars) mice. Where indicated, 10 μM OL (gray bar) was added.

(E) Representative blot of the extent of carbonylation of total colon proteins. Two different samples per condition tested are shown. Protein loading of the samples was verified by western blotting with anti-tubulin antibody. The migration of molecular mass markers is indicated at the left. Arrows (at the right) identify the migration of the two proteins used in the quantification of protein carbonylation (p-40 and p-80 in histograms). The expression of catalase (Cat), SOD2, p-IκBα, and IκBα and the quantification of the p-IκBα/IκBα ratio are also shown.

(F) Glutathione levels in colon extracts from control (CL, closed bar) and I/T (open bar) mice. Bars represent the ratio between reduced and oxidized forms of gluthatione.

(G) Histograms show the MitoP/MitoB ratio in colon from control (CL, closed bar) and I/T (open bar) mice treated or not treated with the mtROS scavenger MitoQ (MQ).

(H) Plasma levels of cytokines in CL (closed bars) and I/T (open bars) mice.

In (A–G), histograms indicate the mean ± SEM of five mice per group assayed in duplicate. *$p < 0.05$, when compared to control by Student's t test.

See also Figure S1A and Table S1.

Metabolic Preconditioning of I/T Mice

In any case, the IF1-mediated inhibition of the H^+-ATP synthase in vivo (Figure 1D) was able to induce metabolic reprogramming of the intestine to an enhanced glycolysis, as revealed by the increased expression of the glycolytic proteins LDH-A and GAPDH (Figure 2A) and data obtained in isolated primary cultures of colonic crypts (Figures 2B–2D). Indeed, and consistent with hIF1 inhibiting the ATP synthase in vivo, colonocytes derived from I/T mice (Figure 2B) presented a reduction in basal and oligomycin-sensitive respiration when compared to controls (Figure 2C), in the absence of any effect on maximal respiration (Figure 2C). Accordingly, I/T colonocytes presented an enhanced glycolysis (Figure 2D) that mimicked the effect of the addition of oligomycin (Figure 2D).

The inhibition of the H^+-ATP synthase by IF1 is known to promote mtROS signaling—both in vivo (Formentini et al., 2014; Santacatterina et al., 2016) and in cells in culture (Formentini et al., 2012; Sánchez-Aragó et al., 2013)—and the subsequent preferential carbonylation of proteins in mitochondria (Figure S1A). Consistently, I/T mice presented enhanced carbonylation of intestinal proteins when compared to littermate controls (Figure 2E). While this is consistent with the generation of mtROS in I/T mice, any such changes were mild, because they did not modify the cellular GSH/GSSG ratio (Figure 2F) and did not activate the expression of SOD2 and catalase (Figure 2E). Consistently, non-significant differences in steady-state levels of mitochondrial hydrogen peroxide were observed in the colons of I/T mice using the exomarker approach (Logan et al., 2014) (Figure 2G). However, activation of the canonical NFκB pathway was shown as the phosphorylation-dependent degradation of its inhibitor IκBα (Figure 2E) (Formentini et al., 2012). Consistent with the activation of the NFκB pathway in the colons of I/T mice, we observed an increase in plasma of interleukin (IL)-6 when compared to controls (Figure 2H). However, we also noted that I/T mice showed significantly lower plasma levels of other pro-inflammatory cytokines, such as IL-1α, IL-1β and G-CSF

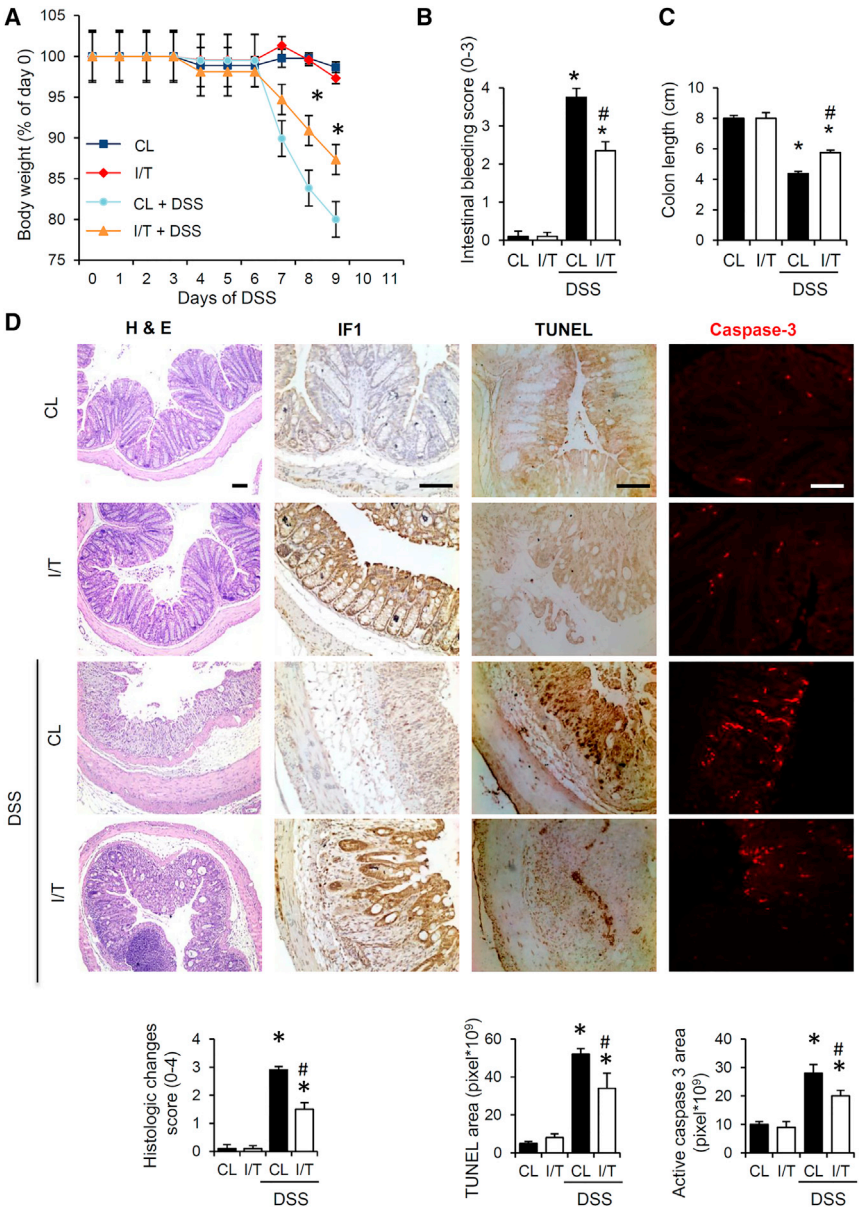

Figure 3. IF1 Expression Protects Colon from DSS-Induced Inflammation

(A) Animal weight is indicated in control (CL, dark and light blue lines) and I/T (red and orange lines) mice at the indicated times after the oral administration of 2% DSS.

(B and C) Histograms show the intestinal bleeding score (B) and colon length (C) in CL (closed bars) and I/T (open bars) mice treated or not treated with 2% DSS during 10 days.

(D) Immunohistochemistry and immunofluorescence microscopy of colons from control (CL) and I/T mice treated or not treated with 2% DSS during 10 days. Colon slices were stained with H&E (first column), anti-IF1 (second column), TUNEL (third column), and anti-active caspase-3 (fourth column). Scale bars, 50 μm.

Histograms show the quantification of the histologic changes score and TUNEL- and active-caspase-3-positive areas in colon slices from CL (closed bars) and I/T (open bars) mice. Histograms indicate the mean ± SEM of six mice per group. *$p < 0.05$, when compared to CL by Student's t test; #$p < 0.05$, when compared to CL+DSS by Student's t test.

See also Figures S1B–S1D.

(granulocyte colony-stimulating factor) (Figure 2H), concurrently with the enhanced plasma expression of the anti-inflammatory cytokine IL-10 (Figure 2H). Expression analysis of markers of immune cell populations, cytokines, and other immune-regulatory and NFκB target genes in the colons of control and I/T mice supported the anti-inflammatory phenotype of I/T mice (Table S1), confirming the enhanced expression of IL-10 and reduction of the pro-inflammatory IL-1β, IL-12, IL-17, and tumor necrosis factor α (TNF-α) (Table S1), thus suggesting that the activation of the NFκB pathway by changes in mitochondrial activity could act as an anti-inflammatory signal in the intestine.

Anti-inflammatory Phenotype of I/T Mice

To investigate this possibility, we followed a standard protocol of DSS-induced colitis (Wirtz et al., 2007). Administration of DSS to the mice induced extensive oxidative damage, as revealed by the nitrosylation and malondialdehyde modification of colon proteins (Figures S1B and S1C). Remarkably, colon extracts of I/T mice experienced less overall oxidative damage than those of controls (Figures S1B and S1C). Consistently, the expression of the transgene significantly reduced the loss in body weight induced by DSS treatment (Figure 3A), partially preventing the inflammation-dependent intestinal bleeding (Figure 3B) and the reduction in colon length (Figure 3C) when compared to controls.

The histological change score, as assessed in H&E-stained sections (Wirtz et al., 2007) (Figure 3D), revealed a significant reduction in I/T mice, indicating that the IF1-mediated inhibition of the ATP synthase confers protection to the colonic epithelium from DSS-induced damage. Accordingly, the estimation of cell death by TUNEL or activated caspase-3 was significantly augmented after 10 days of DSS treatment in control when compared to I/T mice (Figure 3D). These findings suggest that preconditioning afforded by the overexpression of hIF1 in the intestine provides protection against induced colitis. In agreement with previous findings regarding preconditioning in the liver (Santacatterina et al., 2016), we observed a significant induction of Nrf-2 in the colons of I/T mice after DSS administration (Figure S1D).

Signaling the Anti-inflammatory Phenotype

The administration of DSS promoted a stress response in the colons of control and I/T mice, as revealed by the induction of

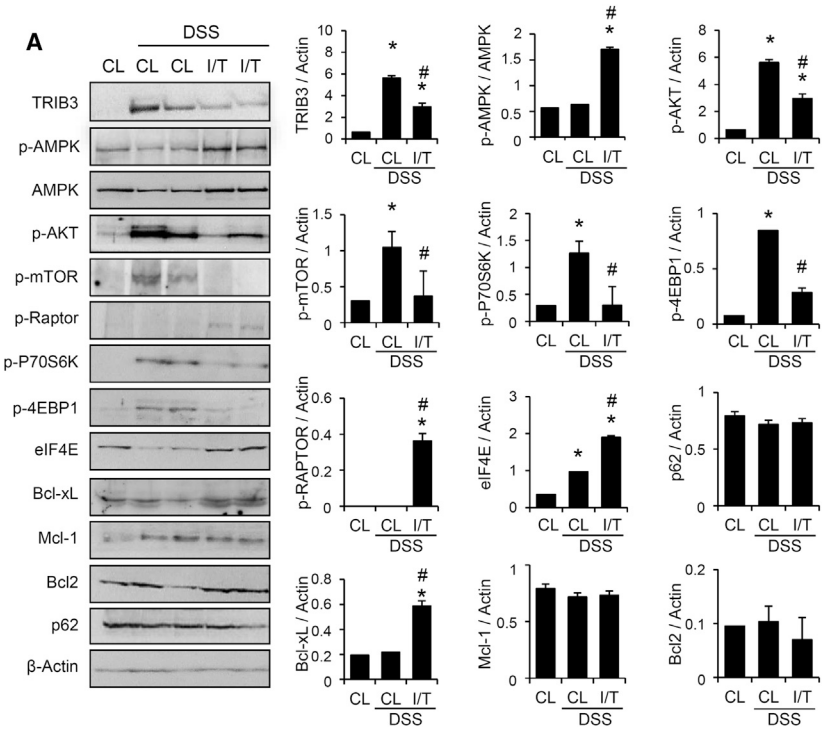

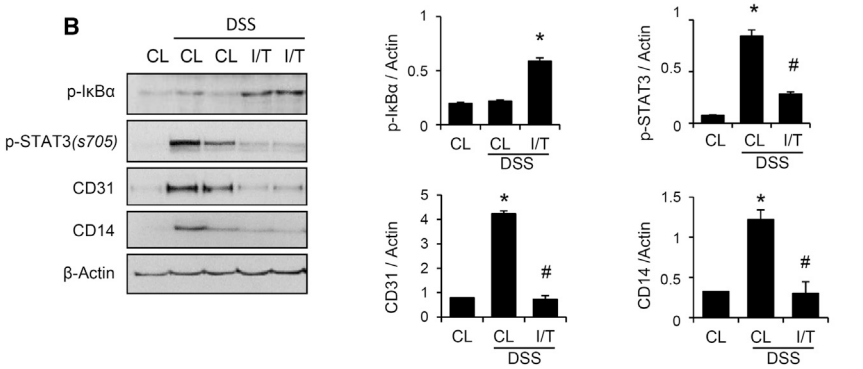

Figure 4. IF1-Mediated Signaling in Response to DSS-Induced Inflammation

(A) Blots show the expression of the stress kinase TRIB3; the metabolic sensor AMPK and p-AMPK; the phosphorylation of AKT (p-AKT) and of proteins of the mTOR pathway (p-mTOR, p-Raptor, p-P70S6K, p-4EBP1, and eIF4E); the anti-apoptotic proteins Bcl-xL, Mcl-1, and Bcl2 and of the autophagy p62 marker.

(B) Same as above showing the phosphorylation of IκBα (p-IκBα) and of STAT3 (p-STAT3); the angiogenic CD31, and invasive CD14 markers in colon extracts from control (CL) and I/T mice before and after 10 days of 2% DSS treatment.

In (A) and (B), one sample of non-treated CL and two different samples of CL and I/T mice after DSS administration are shown. β-actin expression is shown as loading control. Histograms indicate the mean ± SEM of six mice per group and show the relative expression of the indicated protein or ratio referred to control non-treated (CL) or DSS-treated control (CL) and I/T mice. $^{*}p < 0.05$, when compared to CL; $^{\#}p < 0.05$, when compared to DSS-treated CL + DSS by Student's t test, respectively.

See also Figure S2.

the stress kinases TRIB3 and Akt (Figure 4A). However, this response was less pronounced in mice overexpressing hIF1 (Figure 4A). Interestingly, I/T mice, but not control mice, activated the metabolic sensor AMPK (Figure 4A). The activation of Akt in the absence of AMPK activation is known to activate the mTOR pathway, contributing to colon inflammation and cancer progression (Francipane and Lagasse, 2014). Consistently, the colons of I/T mice showed, when compared to controls, a lower activation of the mTOR pathway in response to DSS treatment, as revealed by the lower phosphorylation of mTOR, p70S6K, and 4EBP1 (Figure 4A) and the concurrent enhanced phosphorylation of raptor and eIF4E proteins (Figure 4A). An increase in the expression of the anti-apoptotic Bcl-xL protein in colons of I/T mice was also observed, suggesting that it might contribute to the DSS-resistant phenotype of these animals (Figure 4A). However, no relevant changes in the expression of other anti-apoptotic (Mcl-1 and Bcl-2) and autophagy (p62) markers were observed (Figure 4A).

In agreement with the promotion of an anti-inflammatory phenotype in the colons of I/T mice, despite the NFκB activation observed in these animals (Figure 4B), we observed a lesser activation of the pro-inflammatory STAT3 (Figure 4B), and of the pro-angiogenic and pro-invasive CD31 and CD14 markers, when compared to controls (Figure 4B). Additional markers that emphasize the cell-protective role afforded by the activation NFκB are the maintenance of the expression of the mitochondrial mitofusin 2, OPA1, and VDAC in the colons of I/T mice (Figure S2), suggesting the preservation of mitochondrial integrity in response to the inflammatory stress.

Priming Innate Immunity in I/T Mice

Macrophages are essential components of innate immunity and play key roles in inflammation and disease (Osborn and Olefsky, 2012; Pollard, 2009). Hence, we investigated the inflammatory response and potential polarization of macrophages in DSS-treated animals (Figures 5A and S3). Immunofluorescence analysis of colon tissue slices from I/T and control mice highlighted a significant infiltration of macrophages after DSS treatment in both phenotypes (F4/80+ staining in Figures 5A and S3). We did not observe the co-localization of the macrophage F4/80+ marker and Ki67 in the colons of mice after DSS (Figure S4A), thus supporting that macrophages in the adult mouse intestine do not proliferate and are replenished by recruitment of blood

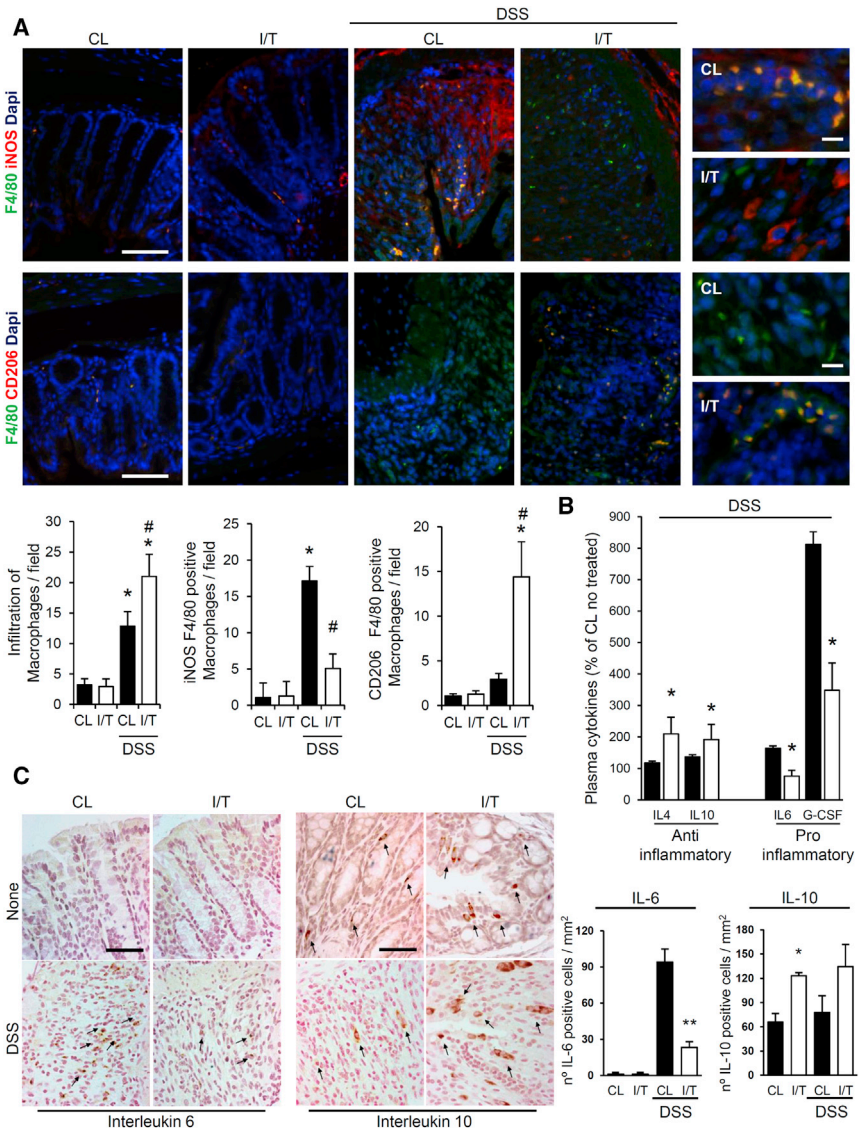

Figure 5. IF1 Mediates Polarization of M2 Macrophages

(A) Immunofluorescence microscopy of macrophages in colons from control (CL) and I/T mice treated or not treated with 2% DSS during 10 days. Upper row: anti-F4/80 (macrophage marker, green), iNOS (M1 macrophage and inflamed tissue marker, red), and DAPI (nuclei, blue). Lower row: anti-F4/80 (green), CD206 (M2 macrophages, red) and DAPI (blue) in control (CL) and I/T mice. Scale bars, 50 μm. (In smaller panels: scale bars, 10 μm). Individual panels are shown in Figure S3. Histograms show the quantification of the total number (F4/80+), M1 (F4/80+/iNOS+), and M2 (F4/80+/CD206+) macrophages per field, respectively. Error bars represent the mean ± SEM of ten fields per condition.

(B) Percent changes in the levels of the anti-inflammatory cytokines IL-4 and IL-10 and in pro-inflammatory cytokines IL-6 and G-CSF in plasma from control (CL, closed bars) and I/T (open bars) mice after 10 days of 2% DSS administration. The data shown indicate the mean ± SEM of seven animals per group.

(C) Immunohistochemistry of colon from control (CL) and I/T mice treated or not treated with 2% DSS during 10 days. Colon slices were stained with anti-IL-6 or anti-IL-10. Scale bars, 50 μm. Arrows indicate positive cells.

Histograms show the number of positive cells per square millimeter in 12 colon slices per condition. In (A) and (B), *$p < 0.05$, when compared to CL by Student's t test; #$p < 0.05$, when compared to CL + DSS by Student's t test. In (C), *$p < 0.05$; **$p < 0.001$, when compared to CL and DSS-treated CL by Student's t test, respectively.

See also Figures S3 and S4.

monocytes (Bain et al., 2014). In colons of control DSS-treated mice, induced nitric oxide synthase (iNOS) expression was augmented, and the infiltrating macrophages were almost all of the M1 phenotype, as revealed by the co-localization of F4/80+ and iNOS staining (Figures 5A and S3). Infiltrating M2 macrophages (F4/80+ and CD206+ cells) were very low in control DSS-treated mice (Figures 5A and S3). Remarkably, the majority of the colon-infiltrating macrophages in DSS-treated I/T mice were of the M2 phenotype, as revealed by the predominant co-localization of F4/80+ and CD206+ staining (Figures 5A and S3), whereas the number of F4/80+, iNOS+ cells was very low (Figures 5A and S3). The lack of F4/80+ and IF1 co-localization (Figure S4B) indicated that IF1 is not being expressed in macrophages, excluding potential cell-extrinsic effects. Consistent with these results, blood cytokines in response to DSS treatment revealed enhanced levels of the anti-inflammatory IL-4 and IL-10 (Figure 5B) and a significant reduction in pro-inflammatory IL-6 and G-CSF (Figure 5B) in I/T mice when compared to controls. Determination of IL-6- and IL-10-positive cells in the colons of control and I/T mice treated with DSS further confirmed the anti-inflammatory phenotype of I/T mice (Figure 5C). Moreover, canonical discriminant analysis using the expression of 17 relevant immune gene markers (Table S1), as selected by the algorithm (B220, CCL2, CD206, CD4, EGR1, NFKB1A, BCL2L1, FOS, CTLA4, ARG1, HMGB1, INHBA, NOS2, IL-10, L13, IL-1β, and NFKB1), revealed that the samples from the four experimental groups nicely clustered into four significantly different groups ($p = 0.005$; Figure 6A).

In line with the anti-inflammatory phenotype of the colons of I/T mice, we observed that CD4+ T cells were most significantly recruited upon treatment with DSS in the colons of I/T mice (Figure 6B). Interestingly, the recruitment of CD4+/FOXP3+ cells (Tregs), those that restrain inflammatory responses, was also significantly augmented in the inflamed colons of I/T mice when compared to those of controls (Figure 6C). Overall, the findings support that the IF1-mediated inhibition of the mitochondrial H^+-ATP synthase in the intestine induces a state of immune preconditioning favoring an anti-inflammatory

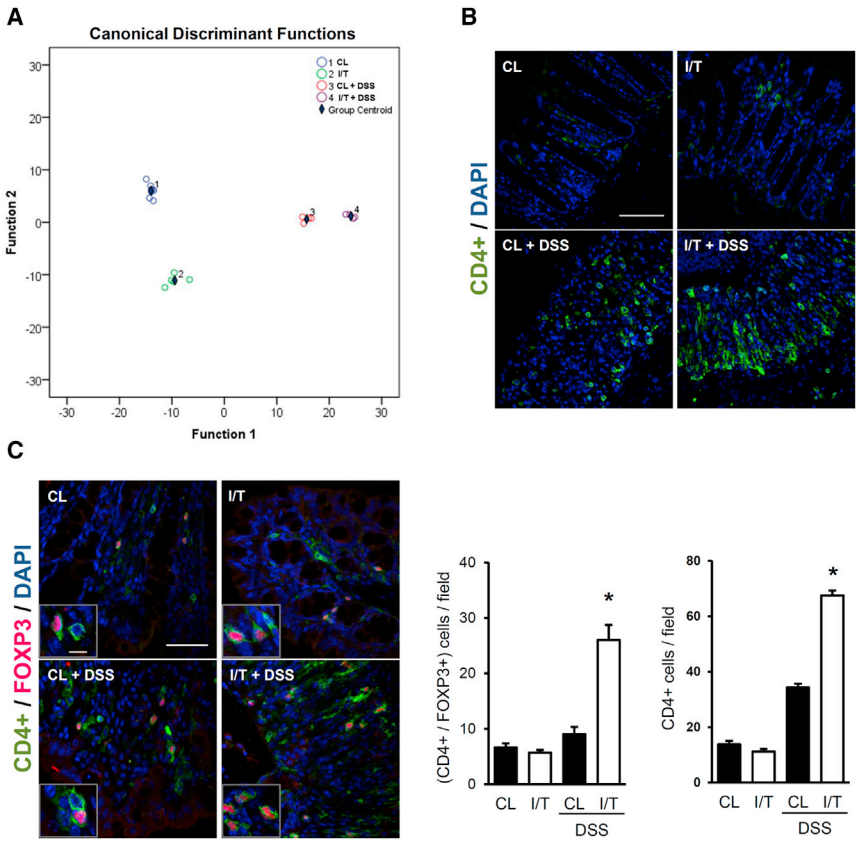

Figure 6. IF1 Mediates the Recruitment of Anti-inflammatory Treg Cells

(A) Gene expression analysis of 46 markers of immune cell populations, cytokines, and other immune-regulatory and NFκB target genes in the colons of CL and I/T mice treated or not treated with DSS (see Table S1). Canonical discriminant analysis using 17 of the genes selected by the algorithm revealed that the samples from control (CL) (1, blue), I/T (2, green), CL + DSS (3, red), and I/T + DSS (4, purple) clustered into four different groups. (B and C) Immunofluorescence microscopy of T cells (CD4+) (B) and Tregs (CD4+/FOXP3+) (C) in colons from control (CL) and I/T mice treated or not treated with 2% DSS during 10 days. Colon slices were stained with anti-CD4 (green), anti-FOXP3 (red), and DAPI (nuclei, blue). Scale bars, 80 μm in (B) and 50 μm in (C); scale bar in inset, 10 μm. Histograms show the number of positive cells per field in 12 colon slices per condition. *$p < 0.001$, when compared to CL+DSS by Student's t test. See also Table S1.

phenotype of the tissue by recruiting M2 macrophages and Treg cells.

Quenching mtROS Blocks the Acquisition of the M2 Anti-inflammatory Phenotype

One potential link between the IF1-mediated decreased colon inflammation in I/T mice is an elevation in mtROS production. To investigate this in vivo, we administered the mitochondria-targeted antioxidant MitoQ to the mice orally as a MitoQ-β-cyclodextrin adduct (Dashdorj et al., 2013). It should be noted that the basal carbonylation of cellular proteins observed in colon extracts was significantly reduced after 10 days of MitoQ administration both in control and in I/T mice (Figure 7A). In line with the finding that MitoQ decreased oxidative stress, MitoQ administration also inhibited the activation of the NFκB pathway in colon extracts of I/T mice (Figure 7B) and abrogated the differences in colon length between control and I/T mice after DSS-induced colitis (Figure 7C). Likewise, histological analysis of the colon after DSS administration and MitoQ treatment revealed no differences between control and IF1-expressing mice (Figure 7D), thus stressing the relevance of mtROS in promoting the phenotypic differences observed. Likewise, the administration of mesalazine, an inhibitor of the NFκB pathway in inflamed intestinal mucosa (Bantel et al., 2000), prevented the phosphorylation of IκBα (Figure 7B) and essentially reproduced the effect of MitoQ treatment in colon length (Figure 7C) and on the histological change scores (Figure 7D). These findings further suggest that the metabolic preconditioning afforded by inhibition of the ATP synthase involves the production of mild-intensity mtROS, which favors an anti-inflammatory phenotype that is effective when the tissue is subsequently challenged with a stressing insult that involves a major production of ROS. In agreement with the aforementioned findings, the IF1-induced mediated polarization of colon macrophages to the M2 phenotype was partially reverted to the M1 phenotype by MitoQ treatment, as revealed by an enhanced iNOS+ staining in the colons of I/T mice (Figure 7E), highlighting mtROS and the NFκB pathway as key mediators in the anti-inflammatory phenotype.

DISCUSSION

Herein, we demonstrate that the expression of hIF1 in the colons of transgenic mice partially inhibits the mitochondrial ATP synthase and promotes the metabolic rewiring of the tissue to an enhanced glycolytic phenotype. Inhibition of the ATP synthase also guides a tissue homeostatic response through the activation of the NFκB pathway by generating the concurrent production of mtROS. We show that the response to acute DSS-induced colitis in control mice is highly aggressive, with elevated plasma levels of the pro-inflammatory cytokines IL6 and G-CSF, the activation of STAT3 and Akt/mTOR pathways, and the functional polarization of tissue macrophages to the M1 pro-inflammatory phenotype. In sharp contrast to the expected pro-inflammatory role of the activation of NFκB in the intestine (Karin and Greten, 2005), the response of transgenic mice to DSS-induced colitis is less aggressive, showing enhanced plasma levels of the anti-inflammatory IL4 and IL10 cytokines, decreases of the pro-inflammatory IL6 cytokine, the activation of AMPK, the polarization of tissue macrophages to the M2 anti-inflammatory phenotype, and the enhanced recruitment of Treg cells that

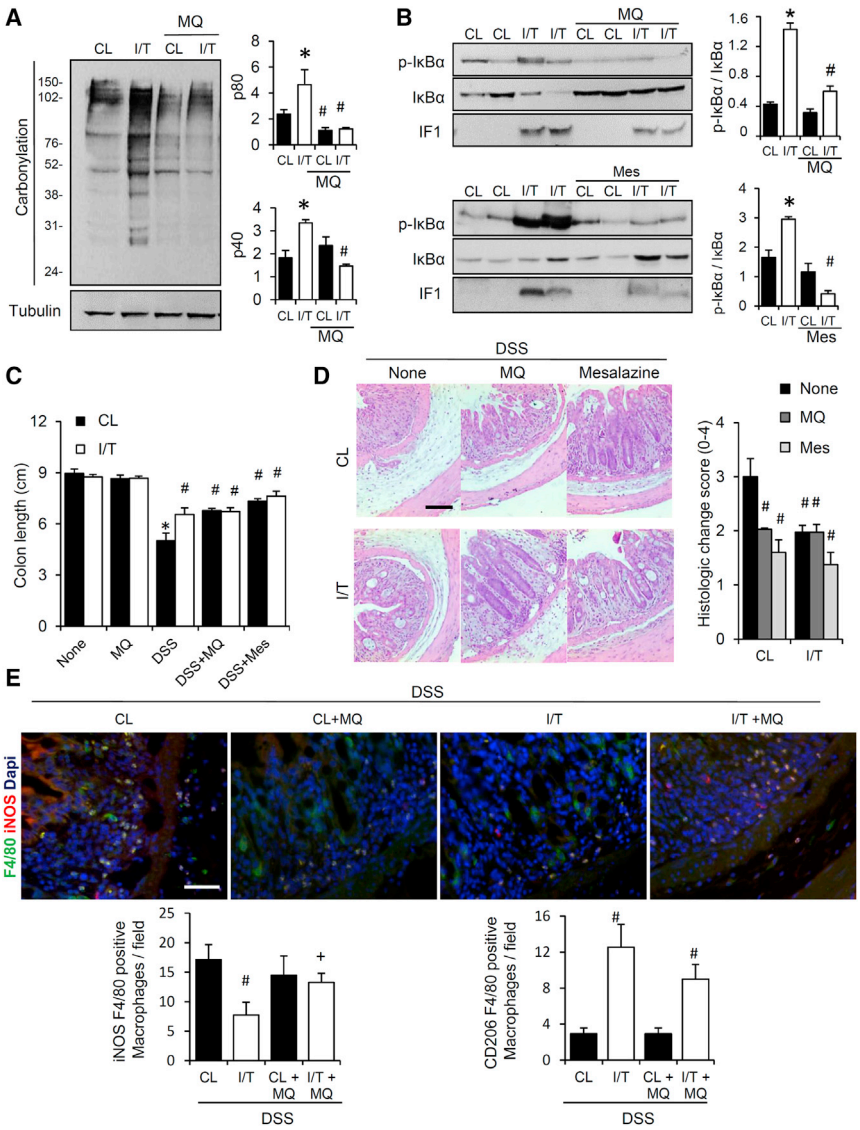

Figure 7. mtROS Guide the IF1-Mediated Protection from Inflammation

Control (CL) and I/T mice were treated or not treated with the mtROS scavenger MitoQ-β-cyclodextrin (MQ) or the NFκB inhibitor mesalazine (Mes).

(A) Representative blot of the extent of protein carbonylation of colon extracts. Tubulin is shown as loading control. The migration of molecular mass markers is indicated at the left. Histograms show the quantification of the carbonylation of p80 and p40 in CL (closed bars) and I/T (open bars) mice treated or not treated with MQ.

(B) Representative blots of phospho-IκBα, IκBα, and human IF1. Two samples per condition tested are shown. Histograms show that expression of IF1 increases the p-IκBα/IκBα ratio in I/T (open bars) when compared to CL (closed bars). MQ treatment and Mes treatment prevent the phosphorylation of IκBα.

(C) Colon length in control (CL, closed bars) and I/T (open bars) mice not treated (None) or treated with MQ, 2% DSS, 2% DSS + MQ, or 2% DSS + mesalazine (DSS+Mes).

(D) H&E of colon slices from control (CL) and I/T mice after treatment with 2% DSS in the absence (None) or presence of MQ or mesalazine. Histograms show the histologic change score in the same conditions. The scale bar represents 50 μm.

(E) Immunofluorescence against F4/80 (green), iNOS (red), and DAPI (blue) in control (CL) and I/T mice after treatment with DSS in the absence or presence of MQ. Scale bar, 50 μm. Histograms show the total number (F4/80+), M1 (F4/80+/iNOS+) and M2 (F4/80+/CD206+) macrophages per field in colon slices from CL (closed bars) and I/T (open bars) mice.

Error bars represent the mean ± SEM of five mice per group. *$p < 0.05$, when compared to CL by Student's t test; #$p < 0.05$, when compared to CL + DSS by Student's t test; +$p < 0.05$, when compared to I/T + DSS by Student's t test.

restrain inflammatory responses. In vivo, the mitochondria-targeted antioxidant MitoQ obliterated the activation of NFκB and its cellular protective effects after the induction of colon inflammation, stressing the relevance of mitochondrial signaling in vivo to the innate immune system of the tissue microenvironment. Overall, these findings emphasize the potential role of the mitochondrial ATP synthase as a therapeutic target in inflammatory and other related diseases.

In vitro findings have suggested a role for IF1 as a unidirectional inhibitor of the ATP hydrolase activity of the mitochondrial ATP synthase (Walker, 2013), especially under conditions of a compromised bioenergetic function of the organelle (Campanella et al., 2008). However, as recently discussed in detail (Formentini et al., 2014; Santacatterina et al., 2016), findings in vivo have shown that IF1 overexpression exerts inhibition of both the synthase activity and hydrolase activity of the enzyme (García-Bermúdez et al., 2015). This contribution, thus, adds an additional in vivo system arguing in the same way.

Consistent with previous findings in cells in culture (Formentini et al., 2012) and in neurons and hepatocytes of the transgenic mice (Formentini et al., 2014; Santacatterina et al., 2016), we observed that the overexpression of IF1 in the colon leads to the carbonylation of some cellular proteins and promotes the activation of the NFκB pathway. In addition, the IF1-mediated signal can be quenched by MitoQ, a mitochondria-targeted antioxidant. Together, these findings are consistent with an mtROS signal, perhaps produced by reverse electron transfer at complex I due to the elevation of the proton motive force that accompanies inhibition of the ATP synthase (Brand et al., 2004). However, as this signal is unable to significantly alter the cellular redox state, it is of mild intensity. mtROS can promote the activation of both the canonical and noncanonical NFκB pathways at various levels. We found that the IF1-mediated NFκB

activation in the colon in vivo is exerted by the canonical pathway, as revealed by the phosphorylation-dependent degradation of the repressor IκBα, in agreement with previous findings in colon cancer cells (Formentini et al., 2012). Despite the activation of NFκB, which is a master regulator of the inflammatory response (Karin, 2006), we noted no relevant phenotypic changes in hIF1-expressing mice when compared to control animals. Phenotypic differences arouse only when I/T mice were challenged with an acute cytotoxic stress. Similar situations have been observed in models of neuronal excitotoxicity and hepatotoxicity using transgenic mice that express the more active IF1-H49K mutant (Formentini et al., 2014; Santacatterina et al., 2016). Thus, these findings support that restraining the activity of mitochondrial OXPHOS, specifically at the ATP synthase level, affords a state of metabolic preconditioning of the tissue that allows cells to withstand further deleterious insults, i.e., mitohormesis (Chandel, 2015; Shadel and Horvath, 2015; Yun and Finkel, 2014). Both genetic (Sun et al., 2014) and metabolic inhibition of the ATP synthase (Chin et al., 2014; Fu et al., 2015) have been shown to propitiate life extension in different organisms. Interestingly, and as is shown in this study, common to these situations is the inhibition of the mTOR pathway and the production of mtROS via reverse electron transport, which are known to extend animal lifespan (Chin et al., 2014; Scialò et al., 2016). Hence, we speculate that the mtROS-mediated activation of the NFkB pathway plays a prominent role in the cellular adaptations that facilitate mitohormesis.

As mentioned earlier, NF-kB signaling represents a key mechanism contributing to gut inflammation and colitis, acting as a central mediator of pro-inflammatory cytokine and chemokine production (Karin and Greten, 2005). To our surprise, but consistent with recent findings that indicate a complex tissue-specific role for the NF-kB pathway in inflammation (Greten et al., 2007; Lawrence et al., 2001; Zhong et al., 2016), the IF1-mediated activation of this pathway in the colons of I/T mice resulted in an anti-inflammatory phenotype. Consistent with our findings, deletion of negative regulators of the NFkB pathway leads to an increased susceptibility to DSS-induced colitis (Garlanda et al., 2004; Lee et al., 2000). Accordingly, we show that reducing the activation of NFκB by the administration of mesalazine is sufficient to abrogate the IF1 anti-inflammatory effect. The activation of autophagy has been shown to be involved in the anti-inflammatory effect of NFkB (Criollo et al., 2010; Zhong et al., 2016). However, we found no relevant changes in p62-guided mitophagy, suggesting that the anti-inflammatory effect of NFkB in our model is exerted by a different mechanism. The preconditioned tissue of transgenic mice responded to DSS administration with a lesser activation of the stress kinase TRIB3 and a diminished cell death, consistent with the negative regulation that the kinase exerts on NFκB, sensitizing cells to TNF- and TRAIL (TNF-related apoptosis-inducing ligand)-induced apoptosis (Wu et al., 2003). Moreover, whereas transgenic mice activated the metabolic stress kinase AMPK in response to DSS-induced colitis, control mice activated the pro-inflammatory and pro-oncogenic STAT3 and Akt/mTOR pathways (Buettner et al., 2002; Francipane and Lagasse, 2014), suggesting that the colons of mice that overexpress hIF1 might be protected from cancer development, compared to control animals. These results might provide a mechanistic explanation to the finding that the overexpression of IF1 in human colon carcinomas is associated with a better patient prognosis (Sánchez-Aragó et al., 2013), while its overexpression in other carcinomas provides a marker of poor patient prognosis (García-Bermúdez and Cuezva, 2016). Interestingly, the colons of I/T mice showed a decreased STAT3 phosphorylation in the context of increased IL6 and IL10. Since both cytokines trigger the phosphorylation of the transcription factor, we suggest that the reduced phosphorylation of STAT3 in the colons of I/T mice might result from the reduced oxidative damage experienced by these animals in response to DSS. In fact, the phosphorylation of STAT3 also depends on the activity of the protein phosphatase Ptp1b, which is known to be inactivated by ROS (Meng et al., 2002). This suggestion agrees well with the observed higher induction of a potential Nrf-2-guided antioxidant response in the colons of the pre-conditioned I/T mice.

Excessive ROS production causes tissue damage. However, a mild ROS production represents a first line of defense against microbial invasion (West et al., 2011), and its suppression reduces innate immune responses (Break et al., 2012). Macrophages are tissue sentinels whose activation is pivotal in restoring tissue integrity and function (Karin and Clevers, 2016). M1 (classically activated) macrophages produce inflammatory cytokines and nitric oxide and are considered more inflammatory (Murray and Wynn, 2011). In contrast, M2 (alternatively activated) macrophages are involved in tissue repair and are considered anti-inflammatory (Murray and Wynn, 2011). M1 and M2 macrophages also differ significantly in the major pathways of energy provision (Mills and O'Neill, 2016) with the adaptations in their mitochondrial respiratory chain playing a relevant role in the antibacterial host defense (Garaude et al., 2016). The source, site, and intensity of the ROS influence the regulation of macrophage signaling and polarization (see Mills and O'Neill, 2016, for a recent review). It has been recently shown that the inhibition of the mitochondrial electron transport chain induces metabolic rewiring of macrophages and controls inflammation by remodeling the Krebs cycle (Lampropoulou et al., 2016). Moreover, other findings also support that lactate, the product of aerobic glycolysis, mediates macrophage polarization from the M1 pro-inflammatory phenotype to the M2 anti-inflammatory phenotype (Colegio et al., 2014). We observed that quenching mtROS production obliterated the activation of NFκB, abolished the advantageous anti-inflammatory phenotype, promoted the increased expression of iNOS, and reduced the recruitment of M2 macrophages or partially suppressed their polarization to the M2 phenotype in the colons of transgenic mice. Since it is unlikely that MitoQ could affect the cell metabolome or the rates of glycolysis imposed by inhibition of the ATP synthase, we suggest that the activation of the NFκB pathway by mtROS in the colons of transgenic mice expressing hIF1 represents the basic mechanism that triggers a higher recruitment and/or polarization of tissue macrophages to the M2 anti-inflammatory phenotype in response to DSS-induced colitis.

Overall, the findings support that the mitochondrial ATP synthase could represent a relevant target to promote macrophage class switching with therapeutic purposes in a number of inflammatory diseases.

EXPERIMENTAL PROCEDURES

Transgenic Animals

The pCMV-SPORT6-IF1 plasmid (ATCC) (Sánchez-Cenizo et al., 2010) containing the human IF1 was PCR amplified, and the PCR product was assembled into the pTRE2hyg vector (Clontech Laboratories) in the BamHI and NotI restriction sites. The TRE2hyg-IF1 plasmid was digested with SexAI/DrdI (New England Biolabs), and the 2.5-kb DNA fragment of interest was purified using the Elu-Quik DNA Purification Kit (Shleicher & Schuell). Transgenic mice (TRE-IF1-47, I) were obtained by pronuclear microinjection of the construct by the Servicio de Trangenesis of the CNB/CBMSO (UAM), using standard protocols. Integration of the construct was confirmed by PCR (forward, 5′-CACAGAGTAGAGAACAACTG-3′; reverse, 5′-GTTAGTAGCACAC AGACAAA-3′). The Villin-rtTA2-M2 mice (T), expressing the transactivator rtTA in intestinal epithelium (Roth et al., 2009) were used. The Tet-On double-transgenic (I/T) animals were obtained by breeding I and T mice (Figure S5A). Animals were maintained on the C57/Bl6 genetic background. To turn on the expression of IF1, 6-month-old double-transgenic mice were administered doxycycline (2 mg/mL) in the drinking water during 15 days (Figure S5B). The same treatment was applied to littermate controls (genotypes I, T, and wild-type) that do not express human IF1 (Figure S5B). Both male and female control and I/T mice were used in the studies. Animal experiments were carried out after approval of the institutional review board (Ethical Committee of the UAM, CEI-52-961) in compliance with animal policies and ethical guidelines of the European Community.

Primary Cultures of Colonocytes

Mature non-dividing epithelial cells forming the colonic epithelium were obtained as previously described (Booth and O'Shea, 2002).

Oxygen consumption rates in isolated colonocytes (500 μg protein) were determined in a Clark-type electrode. TMPD-ascorbate (10 mM) was used as a respiratory substrate in the presence or absence of 0.5 mM ADP, 6 μM oligomycin, 5 μM FCCP, and 1 μM antimycin A.

The rates of lactate production were determined enzymatically, as previously reported (Sánchez-Cenizo et al., 2010).

Determination of the ATP Synthase Activity

Colonocytes resuspended in respiration buffer containing 1% Triton X-100 were used for the spectrophotometric determination of complex V activity, as previously described (Barrientos et al., 2009).

Detection of Inflammatory Cytokines

For the determination of a panel of inflammatory cytokines, the Multi-Analyte ELISArray Kit (QIAGEN) was used.

DSS-Induced Acute Colon Inflammation and Histology

Six-month-old control (n = 18) and I/T (n = 18) doxycycline-treated mice were used (Figure S5B). To induce acute intestinal inflammation, 2% DSS was added in the drinking water for 9 days (Wirtz et al., 2007) in the presence or absence of the anti-inflammatory drug mesalazine (75 mg/kg/day) or the mitochondrial scavenger MS-010 (MitoQ with β-cyclodextrin, 500 μM) simultaneously with doxycycline (Figure S5B). Determination of weight and examination of inflammation-associated rectal bleeding were conducted every day for 10 days. Mice were sacrificed at day 10, and the colons were recollected. Sections (30 μm thick) were taken in the coronal plane, stained with H&E for the evaluation of the histological score (Wirtz et al., 2007), and processed for immunohistochemistry or other analysis.

Western Blot and Analysis of Protein Carbonylation

Protein samples from colons or colonocytes were fractionated on SDS-PAGE. Details of the antibodies used in western blots are provided in Supplemental Information. For the determination of protein carbonylation, the Oxyblot Oxidized Protein Detection Kit (Chemicon International) was used.

Immunohistochemistry

Colon antigens were retrieved by incubation in Dako Retrieval Solution (Dako Cytomation) for 2 min at 98°C. The anti-IF1 (1:50), anti-β-F1-ATPase (1:500), anti-IL10 (Abcam, 1:100), and anti-IL6 (Cell Signaling Technology, 1:20) antibodies were used for immunohistochemistry using the peroxidase-based EnVision FLEX Mini Kit, High pH (Dako Cytomation). Specimens were then incubated with diaminobenzidine chromogenic substrate (Dako Cytomation) for 5 min at room temperature. To assess the rate of cell death, the TUNNEL Kit (Roche) was used.

Immunofluorescence and Confocal Microscopy

Colonocytes or colon slices were incubated with anti-β-catenin (Sigma, 1:500), anti-vimentin (Santa Cruz Biotechnology, 1:500), anti-F4/80 (BioLegend, 1:200), anti-iNOS (BD Transduction Laboratories, 1:200), anti-CD206 (Bio-Rad, 1:200), anti-activated caspase 3 (Cell Signaling Technology, 1:250), anti-Ki67 (Fisher Scientific, 1:100), anti-CD4 (Abcam, 1:200), and anti-FOXP3 (eBioscience, 1:100). TOPRO or DAPI was used to identify nuclei. Secondary Cy-2/Cy-3/Cy-5-conjugated antibodies were used (Millipore Bioscience Research Reagents). Cellular fluorescence was analyzed by confocal microscopy. The area and intensity of fluorescence were quantified by ImageJ software.

Statistical Analysis

Statistical analyses were performed using a two-tailed Student's t test. ANOVAs with post hoc Dunnett's test were used for multiple comparisons to the control, using the SPSS 17.0 software package. The results are indicated as mean ± SEM. A $p < 0.05$ was considered statistically significant.

SUPPLEMENTAL INFORMATION

Supplemental Information includes Supplemental Experimental Procedures, five figures, and two tables and can be found with this article online at http://dx.doi.org/10.1016/j.celrep.2017.04.036.

AUTHOR CONTRIBUTIONS

L.F., F.S., C.N.deA., K.S., D.L.-M., and A.L. performed research; M.F. guided expression analysis of immune genes; R.S. produced and supplied the Villin-rtTA2-M2 mice; M.P.M. produced and supplied mitoQ and mitoB/P probes; L.F. and J.M.C. designed research and analyzed data. J.M.C. wrote the paper. All authors read, contributed to, and approved the final manuscript.

ACKNOWLEDGMENTS

We thank Drs. Laura Sánchez-Cenizo (CBMSO), Ángel L. Corbi (CIB), and María L. Toribio (CBMSO) for their contributions in mouse development, guidance in the selection of macrophage markers, and critical evaluation of the manuscript, respectively. L.F. was supported by the "Fundación de la Asociación Española Contra el Cáncer" (AECC) and the "Ramón y Cajal Program." F.S. and D.L.-M. were supported by FPI-UAM pre-doctoral and MEC-collaboration fellowships, respectively. This work was supported by grants from the MEC (SAF2013-41945-R and SAF2016-75916-R), CIBERER-ISCIII, Comunidad Madrid (S2011/BMD-2402), and Fundación Ramón Areces, Spain. M.P.M. consults for Antipodean Pharmaceutical Inc., which is commercializing MitoQ.

Received: November 7, 2016
Revised: March 3, 2017
Accepted: April 12, 2017
Published: May 9, 2017

REFERENCES

Bain, C.C., Bravo-Blas, A., Scott, C.L., Gomez Perdiguero, E., Geissmann, F., Henri, S., Malissen, B., Osborne, L.C., Artis, D., and Mowat, A.M. (2014). Constant replenishment from circulating monocytes maintains the macrophage pool in the intestine of adult mice. Nat. Immunol. *15*, 929–937.

Bantel, H., Berg, C., Vieth, M., Stolte, M., Kruis, W., and Schulze-Osthoff, K. (2000). Mesalazine inhibits activation of transcription factor NF-kappaB in inflamed mucosa of patients with ulcerative colitis. Am. J. Gastroenterol. *95*, 3452–3457.

Barrientos, A., Fontanesi, F., and Diaz, F. (2009). Evaluation of the mitochondrial respiratory chain and oxidative phosphorylation system using polarography and spectrophotometric enzyme assays. Curr. Protoc. Hum. Genet. *Chapter 19*, Unit19.3.

Booth, C., and O'Shea, J.A. (2002). Isolation and culture of intestinal epithelial cells. In Culture of Epithelial Cells, Second Edition, R.I. Freshney and M.G. Freshney, eds. (Wiley-Liss), pp. 303–335.

Boyer, P.D. (1997). The ATP synthase–a splendid molecular machine. Annu. Rev. Biochem. *66*, 717–749.

Brand, M.D., Affourtit, C., Esteves, T.C., Green, K., Lambert, A.J., Miwa, S., Pakay, J.L., and Parker, N. (2004). Mitochondrial superoxide: production, biological effects, and activation of uncoupling proteins. Free Radic. Biol. Med. *37*, 755–767.

Break, T.J., Jun, S., Indramohan, M., Carr, K.D., Sieve, A.N., Dory, L., and Berg, R.E. (2012). Extracellular superoxide dismutase inhibits innate immune responses and clearance of an intracellular bacterial infection. J. Immunol. *188*, 3342–3350.

Buettner, R., Mora, L.B., and Jove, R. (2002). Activated STAT signaling in human tumors provides novel molecular targets for therapeutic intervention. Clin. Cancer Res. *8*, 945–954.

Campanella, M., Casswell, E., Chong, S., Farah, Z., Wieckowski, M.R., Abramov, A.Y., Tinker, A., and Duchen, M.R. (2008). Regulation of mitochondrial structure and function by the F1Fo-ATPase inhibitor protein, IF1. Cell Metab. *8*, 13–25.

Chandel, N.S. (2015). Evolution of mitochondria as signaling organelles. Cell Metab. *22*, 204–206.

Chin, R.M., Fu, X., Pai, M.Y., Vergnes, L., Hwang, H., Deng, G., Diep, S., Lomenick, B., Meli, V.S., Monsalve, G.C., et al. (2014). The metabolite α-ketoglutarate extends lifespan by inhibiting ATP synthase and TOR. Nature *510*, 397–401.

Colegio, O.R., Chu, N.Q., Szabo, A.L., Chu, T., Rhebergen, A.M., Jairam, V., Cyrus, N., Brokowski, C.E., Eisenbarth, S.C., Phillips, G.M., et al. (2014). Functional polarization of tumour-associated macrophages by tumour-derived lactic acid. Nature *513*, 559–563.

Criollo, A., Senovilla, L., Authier, H., Maiuri, M.C., Morselli, E., Vitale, I., Kepp, O., Tasdemir, E., Galluzzi, L., Shen, S., et al. (2010). The IKK complex contributes to the induction of autophagy. EMBO J. *29*, 619–631.

Dashdorj, A., Jyothi, K.R., Lim, S., Jo, A., Nguyen, M.N., Ha, J., Yoon, K.S., Kim, H.J., Park, J.H., Murphy, M.P., and Kim, S.S. (2013). Mitochondria-targeted antioxidant MitoQ ameliorates experimental mouse colitis by suppressing NLRP3 inflammasome-mediated inflammatory cytokines. BMC Med. *11*, 178.

Formentini, L., Sánchez-Aragó, M., Sánchez-Cenizo, L., and Cuezva, J.M. (2012). The mitochondrial ATPase inhibitory factor 1 triggers a ROS-mediated retrograde prosurvival and proliferative response. Mol. Cell *45*, 731–742.

Formentini, L., Pereira, M.P., Sánchez-Cenizo, L., Santacatterina, F., Lucas, J.J., Navarro, C., Martínez-Serrano, A., and Cuezva, J.M. (2014). In vivo inhibition of the mitochondrial H+-ATP synthase in neurons promotes metabolic preconditioning. EMBO J. *33*, 762–778.

Francipane, M.G., and Lagasse, E. (2014). mTOR pathway in colorectal cancer: an update. Oncotarget *5*, 49–66.

Fu, X., Chin, R.M., Vergnes, L., Hwang, H., Deng, G., Xing, Y., Pai, M.Y., Li, S., Ta, L., Fazlollahi, F., et al. (2015). 2-Hydroxyglutarate inhibits ATP synthase and mTOR signaling. Cell Metab. *22*, 508–515.

Galluzzi, L., Kepp, O., and Kroemer, G. (2012). Mitochondria: master regulators of danger signalling. Nat. Rev. Mol. Cell Biol. *13*, 780–788.

Garaude, J., Acín-Pérez, R., Martínez-Cano, S., Enamorado, M., Ugolini, M., Nistal-Villán, E., Hervás-Stubbs, S., Pelegrín, P., Sander, L.E., Enríquez, J.A., and Sancho, D. (2016). Mitochondrial respiratory-chain adaptations in macrophages contribute to antibacterial host defense. Nat. Immunol. *17*, 1037–1045.

García-Bermúdez, J., and Cuezva, J.M. (2016). The ATPase Inhibitory Factor 1 (IF1): a master regulator of energy metabolism and of cell survival. Biochim. Biophys. Acta *1857*, 1167–1182.

García-Bermúdez, J., Sánchez-Aragó, M., Soldevilla, B., Del Arco, A., Nuevo-Tapioles, C., and Cuezva, J.M. (2015). PKA phosphorylates the ATPase Inhibitory Factor 1 and inactivates its capacity to bind and inhibit the mitochondrial H(+)-ATP synthase. Cell Rep. *12*, 2143–2155.

Garlanda, C., Riva, F., Polentarutti, N., Buracchi, C., Sironi, M., De Bortoli, M., Muzio, M., Bergottini, R., Scanziani, E., Vecchi, A., et al. (2004). Intestinal inflammation in mice deficient in Tir8, an inhibitory member of the IL-1 receptor family. Proc. Natl. Acad. Sci. USA *101*, 3522–3526.

Glancy, B., and Balaban, R.S. (2012). Role of mitochondrial Ca2+ in the regulation of cellular energetics. Biochemistry *51*, 2959–2973.

Gledhill, J.R., Montgomery, M.G., Leslie, A.G., and Walker, J.E. (2007). How the regulatory protein, IF(1), inhibits F(1)-ATPase from bovine mitochondria. Proc. Natl. Acad. Sci. USA *104*, 15671–15676.

Greten, F.R., Arkan, M.C., Bollrath, J., Hsu, L.C., Goode, J., Miething, C., Göktuna, S.I., Neuenhahn, M., Fierer, J., Paxian, S., et al. (2007). NF-kappaB is a negative regulator of IL-1beta secretion as revealed by genetic and pharmacological inhibition of IKKbeta. Cell *130*, 918–931.

Karin, M. (2006). Nuclear factor-kappaB in cancer development and progression. Nature *441*, 431–436.

Karin, M., and Clevers, H. (2016). Reparative inflammation takes charge of tissue regeneration. Nature *529*, 307–315.

Karin, M., and Greten, F.R. (2005). NF-kappaB: linking inflammation and immunity to cancer development and progression. Nat. Rev. Immunol. *5*, 749–759.

Lampropoulou, V., Sergushichev, A., Bambouskova, M., Nair, S., Vincent, E.E., Loginicheva, E., Cervantes-Barragan, L., Ma, X., Huang, S.C., Griss, T., et al. (2016). Itaconate links inhibition of succinate dehydrogenase with macrophage metabolic remodeling and regulation of inflammation. Cell Metab. *24*, 158–166.

Lawrence, T., Gilroy, D.W., Colville-Nash, P.R., and Willoughby, D.A. (2001). Possible new role for NF-kappaB in the resolution of inflammation. Nat. Med. *7*, 1291–1297.

Lee, E.G., Boone, D.L., Chai, S., Libby, S.L., Chien, M., Lodolce, J.P., and Ma, A. (2000). Failure to regulate TNF-induced NF-kappaB and cell death responses in A20-deficient mice. Science *289*, 2350–2354.

Logan, A., Cochemé, H.M., Li Pun, P.B., Apostolova, N., Smith, R.A., Larsen, L., Larsen, D.S., James, A.M., Fearnley, I.M., Rogatti, S., et al. (2014). Using exomarkers to assess mitochondrial reactive species in vivo. Biochim. Biophys. Acta *1840*, 923–930.

Meng, T.C., Fukada, T., and Tonks, N.K. (2002). Reversible oxidation and inactivation of protein tyrosine phosphatases in vivo. Mol. Cell *9*, 387–399.

Mills, E.L., and O'Neill, L.A. (2016). Reprogramming mitochondrial metabolism in macrophages as an anti-inflammatory signal. Eur. J. Immunol. *46*, 13–21.

Murray, P.J., and Wynn, T.A. (2011). Protective and pathogenic functions of macrophage subsets. Nat. Rev. Immunol. *11*, 723–737.

Myant, K.B., Cammareri, P., McGhee, E.J., Ridgway, R.A., Huels, D.J., Cordero, J.B., Schwitalla, S., Kalna, G., Ogg, E.L., Athineos, D., et al. (2013). ROS production and NF-κB activation triggered by RAC1 facilitate WNT-driven intestinal stem cell proliferation and colorectal cancer initiation. Cell Stem Cell *12*, 761–773.

Naik, E., and Dixit, V.M. (2011). Mitochondrial reactive oxygen species drive proinflammatory cytokine production. J. Exp. Med. *208*, 417–420.

O'Neill, L.A. (2014). Biochemistry: succinate strikes. Nature *515*, 350–351.

Osborn, O., and Olefsky, J.M. (2012). The cellular and signaling networks linking the immune system and metabolism in disease. Nat. Med. *18*, 363–374.

Pollard, J.W. (2009). Trophic macrophages in development and disease. Nat. Rev. Immunol. *9*, 259–270.

Quirós, P.M., Mottis, A., and Auwerx, J. (2016). Mitonuclear communication in homeostasis and stress. Nat. Rev. Mol. Cell Biol. *17*, 213–226.

Roth, S., Franken, P., van Veelen, W., Blonden, L., Raghoebir, L., Beverloo, B., van Drunen, E., Kuipers, E.J., Rottier, R., Fodde, R., and Smits, R. (2009). Generation of a tightly regulated doxycycline-inducible model for studying mouse intestinal biology. Genesis *47*, 7–13.

Sánchez-Aragó, M., Formentini, L., Martínez-Reyes, I., García-Bermudez, J., Santacatterina, F., Sánchez-Cenizo, L., Willers, I.M., Aldea, M., Nájera, L., Juarránz, A., et al. (2013). Expression, regulation and clinical relevance of the ATPase inhibitory factor 1 in human cancers. Oncogenesis *2*, e46.

Sánchez-Cenizo, L., Formentini, L., Aldea, M., Ortega, A.D., García-Huerta, P., Sánchez-Aragó, M., and Cuezva, J.M. (2010). Up-regulation of the ATPase inhibitory factor 1 (IF1) of the mitochondrial H+-ATP synthase in human tumors mediates the metabolic shift of cancer cells to a Warburg phenotype. J. Biol. Chem. *285*, 25308–25313.

Santacatterina, F., Sánchez-Cenizo, L., Formentini, L., Mobasher, M.A., Casas, E., Rueda, C.B., Martínez-Reyes, I., Núñez de Arenas, C., García-Bermúdez, J., Zapata, J.M., et al. (2016). Down-regulation of oxidative phosphorylation in the liver by expression of the ATPase inhibitory factor 1 induces a tumor-promoter metabolic state. Oncotarget *7*, 490–508.

Scialò, F., Sriram, A., Fernández-Ayala, D., Gubina, N., Lõhmus, M., Nelson, G., Logan, A., Cooper, H.M., Navas, P., Enríquez, J.A., et al. (2016). Mitochondrial ROS produced via reverse electron transport extend animal lifespan. Cell Metab. *23*, 725–734.

Sena, L.A., and Chandel, N.S. (2012). Physiological roles of mitochondrial reactive oxygen species. Mol. Cell *48*, 158–167.

Shadel, G.S., and Horvath, T.L. (2015). Mitochondrial ROS signaling in organismal homeostasis. Cell *163*, 560–569.

Shi, L., and Tu, B.P. (2015). Acetyl-CoA and the regulation of metabolism: mechanisms and consequences. Curr. Opin. Cell Biol. *33*, 125–131.

Sun, X., Wheeler, C.T., Yolitz, J., Laslo, M., Alberico, T., Sun, Y., Song, Q., and Zou, S. (2014). A mitochondrial ATP synthase subunit interacts with TOR signaling to modulate protein homeostasis and lifespan in Drosophila. Cell Rep. *8*, 1781–1792.

Walker, J.E. (2013). The ATP synthase: the understood, the uncertain and the unknown. Biochem. Soc. Trans. *41*, 1–16.

Weinberg, S.E., Sena, L.A., and Chandel, N.S. (2015). Mitochondria in the regulation of innate and adaptive immunity. Immunity *42*, 406–417.

West, A.P., Brodsky, I.E., Rahner, C., Woo, D.K., Erdjument-Bromage, H., Tempst, P., Walsh, M.C., Choi, Y., Shadel, G.S., and Ghosh, S. (2011). TLR signalling augments macrophage bactericidal activity through mitochondrial ROS. Nature *472*, 476–480.

West, A.P., Khoury-Hanold, W., Staron, M., Tal, M.C., Pineda, C.M., Lang, S.M., Bestwick, M., Duguay, B.A., Raimundo, N., MacDuff, D.A., et al. (2015). Mitochondrial DNA stress primes the antiviral innate immune response. Nature *520*, 553–557.

Wirtz, S., Neufert, C., Weigmann, B., and Neurath, M.F. (2007). Chemically induced mouse models of intestinal inflammation. Nat. Protoc. *2*, 541–546.

Wu, M., Xu, L.G., Zhai, Z., and Shu, H.B. (2003). SINK is a p65-interacting negative regulator of NF-kappaB-dependent transcription. J. Biol. Chem. *278*, 27072–27079.

Yun, J., and Finkel, T. (2014). Mitohormesis. Cell Metab. *19*, 757–766.

Zhong, Z., Umemura, A., Sanchez-Lopez, E., Liang, S., Shalapour, S., Wong, J., He, F., Boassa, D., Perkins, G., Ali, S.R., et al. (2016). NF-κB restricts inflammasome activation via elimination of damaged mitochondria. Cell *164*, 896–910.